

Recent Progress in Power Generation from Water/Liquid Droplet Interaction with Solid Surfaces

Wei Tang, Bao Dong Chen, and Zhong Lin Wang*

Water covers $\approx 70\%$ of the Earth's surface and it contains a tremendous amount of energy that remains unexploited. With the advance of nanotechnology, new strategies toward harnessing water energy based on new mechanisms are proposed. Here, the interaction mechanisms between a water droplet and a solid surface for harvesting energy, including water–solid contact electrification in the four basic working modes of a triboelectric nanogenerator and streaming current, are reviewed. Among them, nanogenerators based on the contact electrification show the highest output. Practical applications are also presented, such as sensing application, wearable power generation, all-weather power generation, and blue energy solutions. At last, perspectives and opportunities for using water/liquid-based energy are discussed.

1. Introduction

Water covers over 70% of the Earth's surface. It not only supports life, but also contains tremendous energy. The water energy involves a variety of forms, including chemical, thermal, kinetic, and so on. The chemical energy is widely exploited, such as water splitting by electricity^[1] or photocatalysis.^[2] The thermal energy is utilized for salinity power generation.^[3] The kinetic energy is well developed as hydropower, which is widely distributed and of high economic value.

In the recent years, with the advance of nanotechnology and nanoscale materials, new strategies toward harnessing the

water kinetic energy are proposed. Based on the water–solid contact electrification, Lin et al. reported a water-based triboelectric nanogenerator (TENG).^[4] The TENG is newly invented by Wang's group,^[5–7] which is dominated by the displacement current derived from the Maxwell equation.^[8,9] It is based on the combining of contact electrification and the electrostatic induction effect,^[10–15] and featured with low cost, significant high output, and diverse material choices,^[16–22] making it suitable for water kinetic energy harvesting. Researchers all over the world are focusing on this field.^[23–28] Four basic working modes are classified and recalled

in this review. Subsequently, the streaming potential/current is discussed. After Quincke first discovered this effect in 1859, in powdered glass, ivory chips, graphite, and so on,^[29,30] Dekker and co-workers^[31] and Wang and co-workers,^[32] respectively, investigated this phenomenon and proposed the streaming current generator. Moreover, Fan and co-workers^[33] and Guo and co-workers^[34–36] studied the streaming current generator on thin films. Furthermore, some other water kinetic harvesters are also introduced.

As for the applications, we systematically review and list many newly developed self-powered applications, including fluidic sensors,^[37–39] inertial sensors,^[40] and self-powered metal anticorrosion^[41] and antibiobouling.^[42] Most of them are based on the TENG mechanism. In addition, owing to the deformability of the fluid and the flexibility of the TENG, the liquid-based triboelectric nanogenerator (L-TENG) is superflexible, making it suitable for portable and wearable applications.^[43,44] Moreover, the L-TENG is demonstrated to harvest energy from natural water, including rain drops,^[45,46] wave,^[47,48] and even underwater ultrasonic vibrations,^[49] which makes it feasible to develop an all-weather energy harvester and serve as a unique solution to blue energy.^[50,51] At last, we discuss about perspectives and opportunities for future development and applications.

2. Liquid Energy Harvesting Based on Water–Solid Contact Electrification

As we know, contact electrification exists everywhere, which is the fundamental principle of the newly invented triboelectric nanogenerator.^[52] As the TENG's two tribo materials separate, the two surfaces possess opposite charges, which will build up an electric potential difference on the two back electrodes

Dr. W. Tang, Dr. B. D. Chen, Prof. Z. L. Wang
CAS Center for Excellence in Nanoscience
Beijing Key Laboratory of Micro–Nano Energy and Sensor Beijing
Institute of Nanoenergy and Nanosystems
Chinese Academy of Sciences
Beijing 100083, P. R. China
E-mail: zhong.wang@mse.gatech.edu

Dr. W. Tang, Dr. B. D. Chen, Prof. Z. L. Wang
School of Nanoscience and Technology
University of Chinese Academy of Sciences
Beijing 100049, P. R. China

Dr. W. Tang, Prof. Z. L. Wang
Center on Nanoenergy Research
School of Physical Science and Technology
Guangxi University
Nanning 530004, P. R. China

Prof. Z. L. Wang
School of Material Science and Engineering
Georgia Institute of Technology
Atlanta, GA 30332, USA

 The ORCID identification number(s) for the author(s) of this article can be found under <https://doi.org/10.1002/adfm.201901069>.

DOI: 10.1002/adfm.201901069

(Figure 1a). When a load is connected, a current will form, flowing from one electrode to the other, in order to screen up the electric field formed by the separated charged surfaces. When two surfaces are brought into contact again, the potential difference on the two electrodes will change, leading to a current flowing backward. Therefore, an alternative current (AC) is observed by repeating this cycle.

2.1. Contact–Separation Mode TENG

Lin et al. reported a contact–separation-mode L-TENG in Figure 2a.^[4] The water is utilized as the dielectric material, contacting with polydimethylsiloxane (PDMS). The working mechanism is explained as that, when the water contacts with PDMS, PDMS will be negatively charged due to the ionization of the surface group, whereas the water is positively charged. As the PDMS and water separate, tribo charges in the interface will induce the electrons in the external circuit moving from the back electrode of PDMS to that of the water. When the PDMS approaches to the water, the electrons move backward. Therefore, an alternative current is obtained in the external circuit under the mechanical triggering. It is found that the deionized (DI) water gives the highest output, with a charge density of $31.3 \mu\text{C m}^{-2}$. As a comparison, the tap water gives $15.02 \mu\text{C m}^{-2}$, and the NaCl solution (0.6 M) gives $5.7 \mu\text{C m}^{-2}$ (Figure 2b). This result suggests that, after contact electrification, an electrostatic field is formed on the solid film's surface, which will attract the counterions in the water, if exists, forming the electrical double layer (EDL) to screen its surface charges. More moveable ions are there in the water, much heavily the charges on the solid surface are screened. Therefore, DI water shows the highest output performance. Moreover, as the water's temperature increases, the output of the device decreases, corresponding to the above explanation. Additionally, the output of the L-TENG by using water is compared with those by using organic solvent (such as glycerin, ethanol, isopropyl alcohol, and *n*-hexane) (Figure 2c).^[53] The results show that the water gives the highest output, indicating that a higher polarity of the liquid will generate a better electrification performance, and thus leads to a larger output.

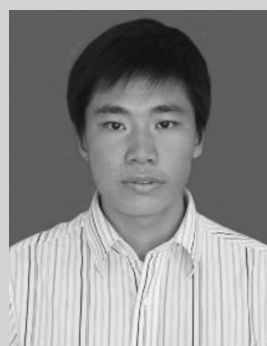
2.2. Sliding Mode TENG

The second mode for the L-TENG is the sliding mode, as shown in Figure 3. Here, the liquid metal is selected, serving as the metal part, contacting with the dielectric material. Figure 3a shows the configuration of the device.^[54] When the dielectric material of polytetrafluoroethylene (PTFE) contacts with a liquid metal, electrons are injected to the PTFE's surface due to the difference of electron-attracting ability for the PTFE and the liquid metal. As the PTFE moves up, the tribo charges on the surface will drive the electrons to move from its induction electrode (the blue part) to the liquid metal through the external circuit. When the PTFE moves back into the liquid metal, the electrons move backward. Figure 3b illustrates the electrical characterization between the liquid metal and various solid films. Except PDMS, all



Wei Tang is an associate professor at the Beijing Institute of Nanoenergy and Nanosystems, Chinese Academy of Sciences. He received his B.S. and Ph.D. degrees from the School of Physics and School of Electronics Engineering and Computer Science in 2008 and 2013, respectively, from Peking University, China. His

research interests include triboelectric nanogenerators, self-powered systems and wireless sensing networks, and micro/nanoengineering.



Baodong Chen is an associate professor at the Beijing Institute of Nanoenergy and Nanosystems, Chinese Academy of Sciences. He received his Ph.D. degree from the School of Materials Science and Engineering in 2015 from Inner Mongolia University of Technology, China. His research interests

include triboelectric nanogenerators, self-powered systems, and 2D- and 3D-printed flexible electronics.



Zhong Lin Wang is the Hightower Chair in Materials Science and Engineering and Regents' Professor at Georgia Tech, and the chief scientist and director of the Beijing Institute of Nanoenergy and Nanosystems, Chinese Academy of Sciences. His discovery and breakthroughs

in developing nanogenerators and self-powered nanosystems establish the principle and technological road map for harvesting mechanical energy from environmental and biological systems for powering personal electronics and future sensor networks. He coined and pioneered the field of piezotronics and piezophotonics.

the polymer films, including PTFE, Kapton, PET, polyvinyl chloride (PVC), Perylene, show high charge density above $200 \mu\text{C m}^{-2}$. In particular, Kapton film with a thickness of $50 \mu\text{m}$ achieves a high density of $400 \mu\text{C m}^{-2}$, which is several times bigger than any other reported value at that time. This result shows that the liquid metal with electrons as the carriers works well in the liquid–solid contact electrification.

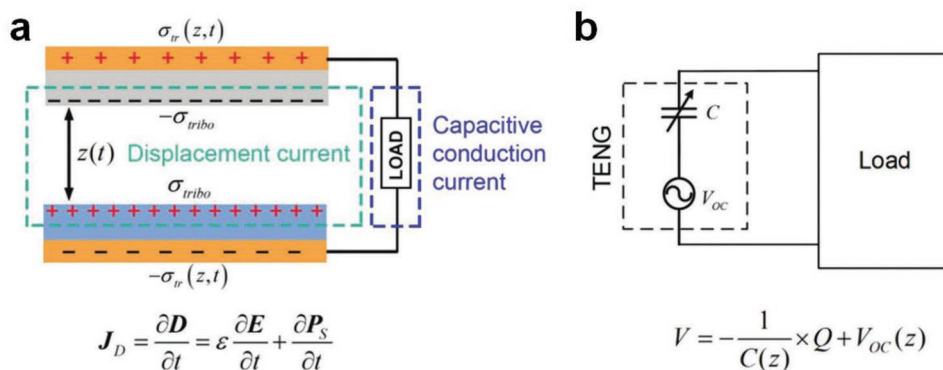


Figure 1. a) Schematic of the working mechanism of the triboelectric nanogenerator. b) The equivalent circuit of the TENG. Reproduced with permission.^[52] Copyright 2018, Wiley-VCH.

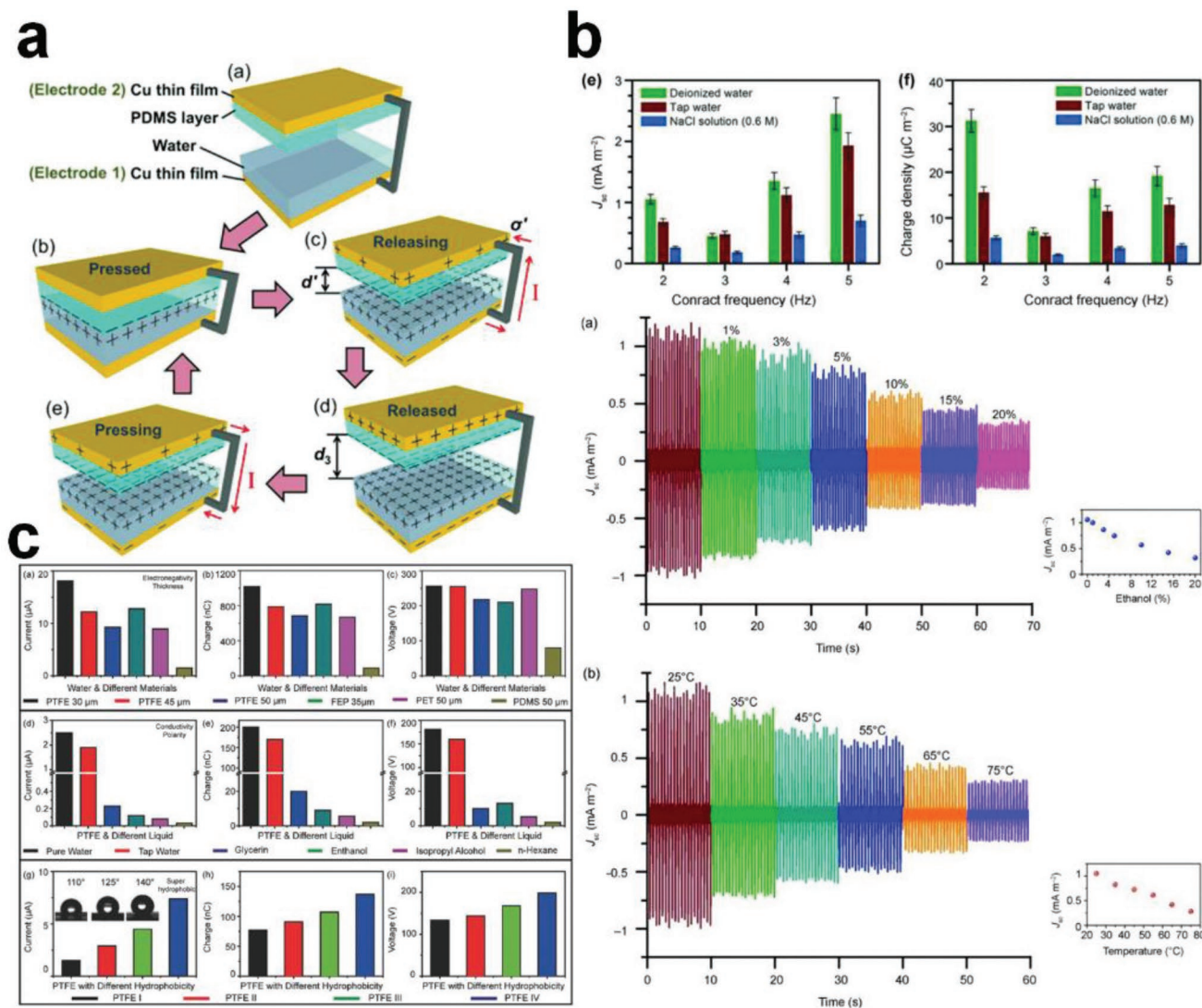


Figure 2. a) Contact–separation mode of TENG. b) Electrical characterization of the TENG. Reproduced with permission.^[4] Copyright 2013, Wiley-VCH. c) Output performance under various materials and liquids. Reproduced with permission.^[53] Copyright 2018, Wiley-VCH.

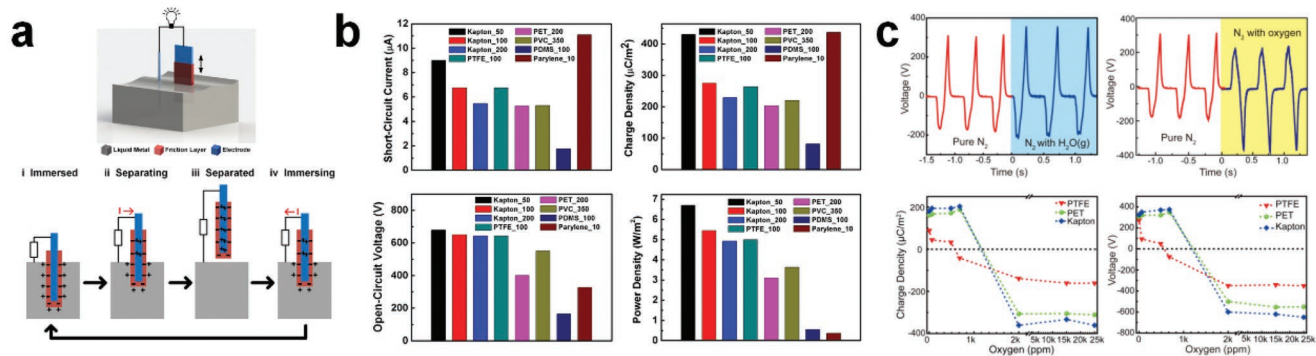


Figure 3. a) Sliding-mode L-TENG, with a liquid metal as the contacting metal. b) Output performance under various materials. Reproduced with permission.^[54] Copyright 2015, Wiley-VCH. c) The influence of the gas condition. Reproduced with permission.^[55] Copyright 2017, AIP Publishing.

Additionally, the liquid metal–based contact electrification is investigated in different gas environments.^[55] It is found that oxygen significantly influences the contact electrification process. The Kapton is negatively charged by the liquid metal when exposed to the oxygen, whereas it is positively charged without oxygen, as shown in Figure 3c. It implies that gas molecules play an important role in the liquid–solid contact electrification.

2.3. Single-Electrode Mode TENG

Figure 4 shows the single-electrode mode of the L-TENG. Here, the water serves as a moving part. Two roles might be played by the water. As shown in Figure 4a,^[45] when the water droplet is charged initially (normally positively by air or the pipe^[56–58]), it will induce negative charges in the induction electrode (the orange part), which is covered by PTFE. If the water droplet is

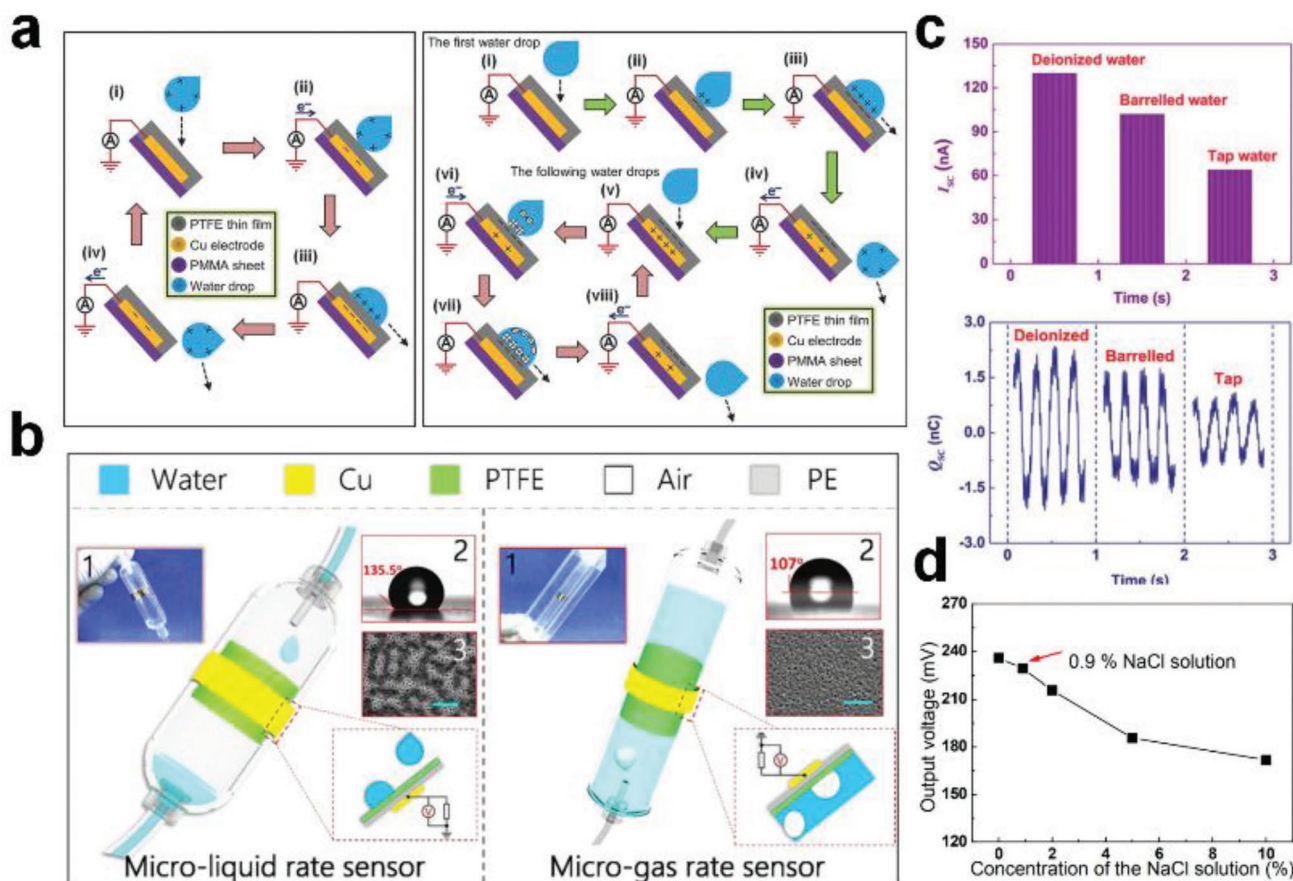


Figure 4. a) The single-electrode-mode L-TENG. Reproduced with permission.^[45] Copyright 2014, Wiley-VCH. b) The configuration of microliquid flow detection. Reproduced with permission.^[59] Copyright 2016, American Chemical Society. c,d) The L-TENG's output depending on the ionic concentration. Reproduced with permission.^[38] Copyright 2017, Wiley-VCH.

free of charge, it will contact with PTFE and eventually negatively charged the surface of the film. When it leaves off the surface, the negative charges will drive electrons in the back electrode of the film to move into the ground, in order to achieve an electrostatic equilibrium, forming a current flowing from the ground to the device. As the next water drop approaches the film, the charges on the surface will attract and realign the electric dipole moment in the water, which will drive the positive holes to move into the ground, obtaining a new equilibrium. Hu and co-workers utilized this mechanism in the channel of infusion system.^[59] The triboelectrification signals will be generated from the droplet via the capillary, showing a good response to the infusion process. Chen et al. reported a capillary-tube L-TENG, which shows a high sensitivity to detect a 0.5 μL liquid droplet (Figure 4c).^[38] Figure 4d shows that the water gives higher output compared to the ionic solutions, corresponding to the explanation we discussed above. Moreover, the results show a promising application potential in the micrototal analysis system (μTAS) for the single-electrode-mode L-TENG.

2.4. Freestanding-Mode TENG

The fourth mode of the L-TENG is the freestanding mode, as presented in Figure 5a.^[47] Zhu and co-workers reported this device to harvest the fluctuation energy of the water wave. After repetitive frictions, the surface of the fluorinated ethylene propylene (FEP) is negatively charged. When the water moves up and down, the electric dipole moment will screen negative charges on the FEP and induce electrons to move forth and

back between electrodes A and B (Figure 5b). Additionally, they upgraded the design, by dividing the electrode into many columns (Figure 5c),^[48] making each electrode work as a single TENG device. Therefore, any tiny fluctuation from water wave could be harvested, as shown in Figure 5d. The device's output is demonstrated to reach 300 V and 15 μA . And it can power up a wireless signal transmitter, which is promising for water quality wireless monitoring in rivers or oceans.

3. Liquid Energy Harvesting Based on Streaming Current

The streaming current is known for a long time, which is caused by the electric double layer. According to the Gouy–Chapman model, when a solid exposed to a liquid, two charge layers will be formed (Figure 6). The inner layer, called as the stern layer, refers to ions adsorbed onto the solid surface. The outer layer, called as the diffuse layer, contains mobile counterions, to screen up the inner layer. The ions in this layer is loosely associated with the solid and will move with the liquid. Therefore, under an external driving force, an ion flow-induced electrical current is obtained, named with the streaming current, if there is a pressure difference or concentration difference.^[60,61]

3.1. Streaming Current in Channels

Streaming potential/current was discovered decades ago.^[29] With the advance of the nanotechnology, Stein and co-workers^[31] first

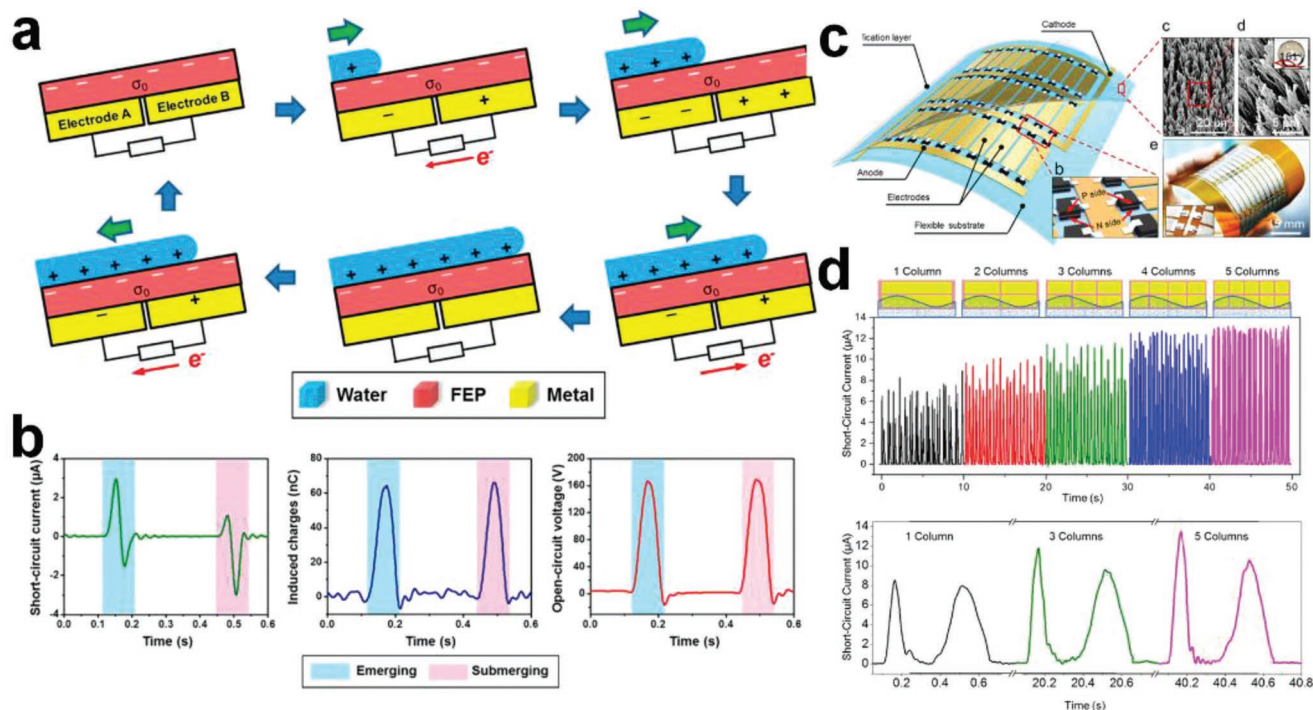


Figure 5. a,b) Freestanding-mode L-TENG and its electrical characterization. Reproduced with permission.^[47] Copyright 2014, American Chemical Society. c,d) The networked-integrated L-TENG and the electrical characterization. Reproduced with permission.^[48] Copyright 2018, American Chemical Society.

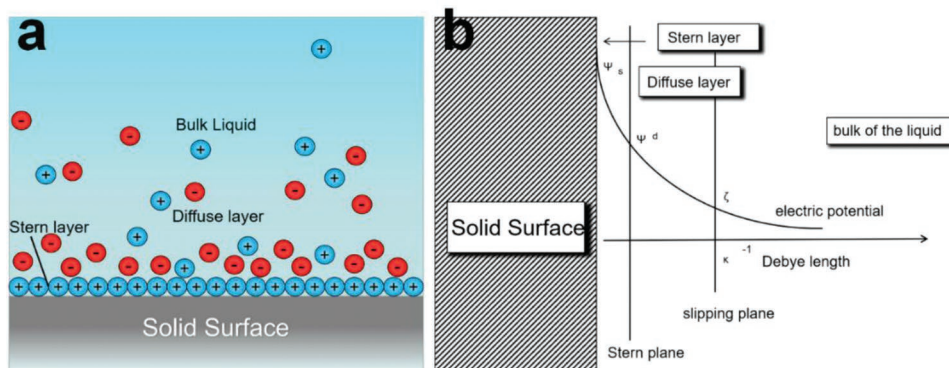


Figure 6. a) The schematic of the water–solid interface. b) The electric double layer.

investigated this by fabricating a silica nanochannel with 70 nm in height, 50 μm in width, and 4.5 mm in length (Figure 7a). Under a driven pressure of 1 bar, the device outputs about 10 pA constantly within a low salt concentration, but dramatically decreases when the concentration is above 10×10^{-3} M. Zhang et al.^[32] proposed a streaming current generator with a macroscopic channel and porous patterns (Figure 7b). Compared to the traditional nanochannels, their design possesses larger dimension and more flux. It is found to provide an output current of 1.75 nA, with the potassium chloride (KCl) solution's concentration of 1×10^{-6} M and a flow velocity of 0.4 mL min^{-1} . Moreover, it is utilized to power a single-nanowire pH sensor.

3.2. Streaming Current on Thin Films

Besides in micro/nanochannels, according to the literature, streaming current can also be observed on thin films, such as graphite.^[29,30] Therefore, a variety of materials with

micro/nanostructures should work. Figure 8a shows Fan's work by employing porous carbon nanotube/polyaniline composite (CNT/PANI) and poly(vinyl alcohol) (PVA) gel.^[33] The porous PVA gels provides many narrow channels, with CNT/PANI electrodes surrounded, and meanwhile, the PVA chains will attract H^+ but repulse negative ions. Therefore, when the water passes through, the film will allow negative ions to pass but block positive ions like H^+ , resulting in a streaming current. As reported, a sandwich device can output a current of 1.65 mA, with a voltage about 150 mV. Guo and co-workers also reported several devices based on thin film structure, made up of the graphene.^[34–36] Figure 8b shows a graphene sheet immersing in the water. As the sheet moves up and down, electricity is generated. It is found that this waving device can produce a voltage about 100 mV, and a current of 11 μA , with a moving velocity of 1 m s^{-1} and a sheet size of 20 cm^2 . Afterward, a falling droplet configuration is developed, as shown in Figure 8c. By placing a monolayer graphene on the PET, the device can achieve 100 mV and 10 μA .

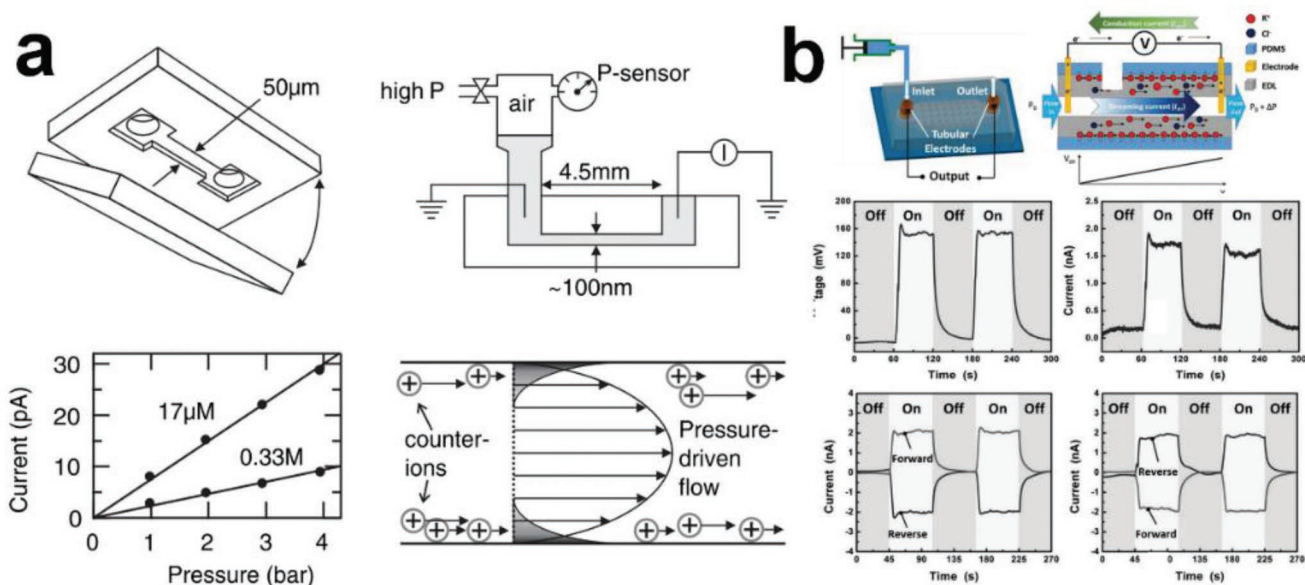


Figure 7. a) The streaming current in a silica nanochannel. Reproduced with permission.^[31] Copyright 2005, American Physical Society. b) A streaming current generator. Reproduced with permission.^[32] Copyright 2015, Wiley-VCH.

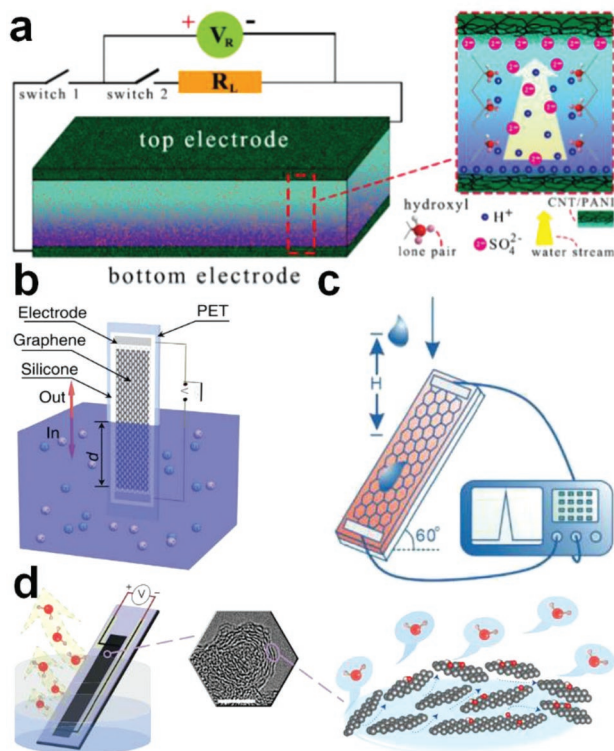


Figure 8. a) Streaming current in CNT/PANI and PVA gel. Reproduced with permission.^[33] Copyright 2018, American Chemical Society. b,c) Streaming current on the graphene. Reproduced with permission.^[34] Copyright 2014, Macmillan Publishers Limited. Reproduced with permission.^[35] Copyright 2018, American Chemical Society. d) Streaming current induced by water evaporation on the carbon black. Reproduced with permission.^[62] Copyright 2017, Spring Nature Publishing AG.

Additionally, Zhou and co-workers proposed a water-evaporation configuration with the nanostructured carbon black as the substrate.^[62] As the water evaporates, leaving off the surface,

the streaming current is formed accordingly. It is found that the evaporation on centimeter-sized carbon black can output a sustained voltage of 1 V and a current about 100 nA. It is worth mentioning that, during the evaporation process, the thermal energy is involved.

4. Liquid Energy Harvesting Based on Other Mechanisms

Since the water/liquid could be conductive, some other types of generators are proposed, based on the triboelectric nanogenerator, with the liquid as the electrode. The one shown in **Figure 9a** simply consists of a rubber sleeve with a conductive liquid (NaCl solution).^[43] It works in the single-electrode mode of the traditional TENG with the NaCl solution serving as an induction electrode, and outputs 67.7 V and 35 nC, when periodically tapped by the nylon film. At a match load of 300 M Ω , this device achieves 200 W m⁻² under a frequency of 3 Hz. More importantly, it is superflexible, and maintain the output performance even under a strain as large as 300%. Lee and co-workers developed a superstretchable L-TENG, based on the liquid metal (Galinstan).^[44] Operating in the single-electrode mode with a frequency of 3 Hz, the device possessing an area of 6 \times 3 cm² outputs 354.5 V, 123.2 nC, and 15.6 μ A, with a power density around 8.43 mW m⁻². In addition, Helseth also reported a flexible and stretchable L-TENG, by using interdigital electrodes, with the liquid metal encapsulated in elastomers.^[63]

Xi et al. presented a TENG employing spherical pellets as the media to perform the contact–separation process driven by the underwater ultrasonic wave (**Figure 10**). The device outputs a current about one hundred milliamps, and achieves a power of 0.362 W cm⁻², under an ultrasonic wave frequency of 80 kHz. The power conversion efficiency is found to be as high as 13.1%. The equivalent output galvanostatic current is 1.43 mA. This device is able to continuously light up to 12 lamps, and drive

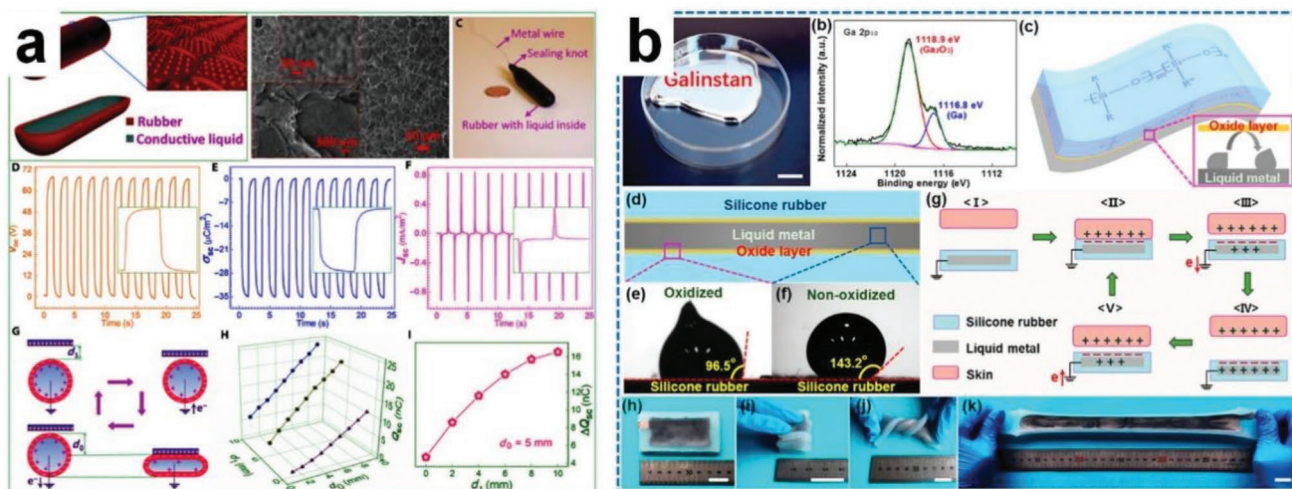


Figure 9. a) L-TENG by using the conductive solution as the induction electrode. Reproduced under the terms and conditions of the Creative Commons Attribution-NonCommercial License.^[43] Copyright 2016, The Authors, published by AAAS. b) L-TENG by using the liquid metal as the induction electrode. Reproduced with permission.^[44] Copyright 2018, American Chemical Society.

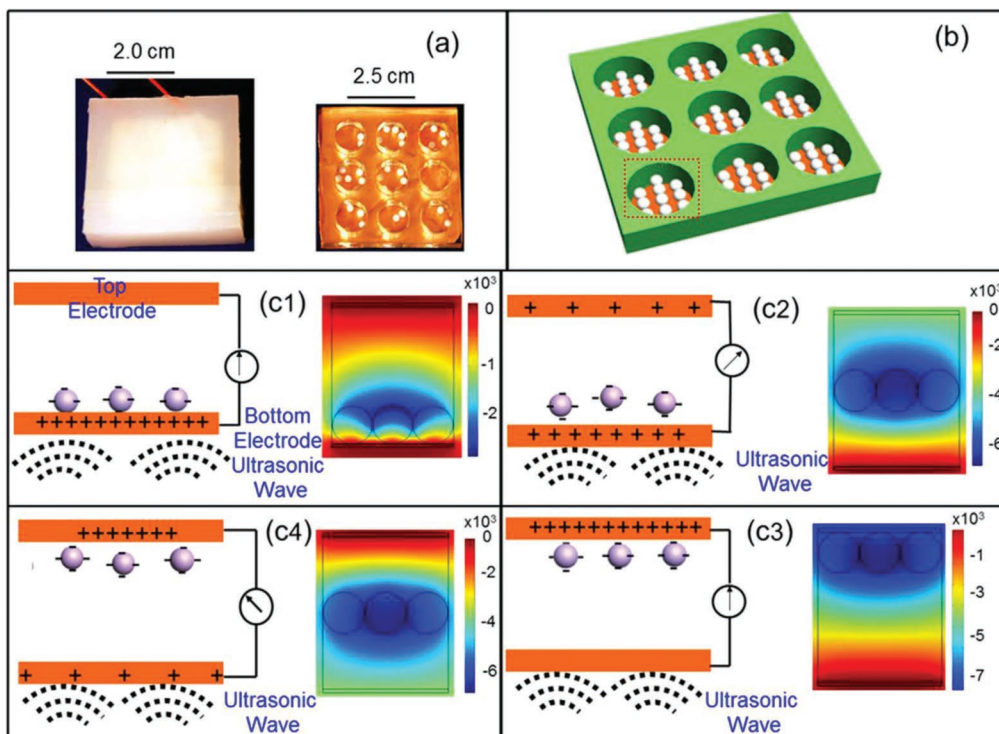


Figure 10. TENG targeting for the underwater ultrasonic vibration. Reproduced with permission.^[49] Copyright 2017, Elsevier.

an electronic watch and a temperature/humidity meter, which shows an outstanding potential for underwater applications.

Some other devices for the water kinetic energy harvesting are investigated, based on photon coupling or Coulombic scattering. In brief, it is reported that, for metallic tubes, free electrons are mostly driven by hot phonons around the tube walls, caused by the friction of the moving liquid, as opposed to the carrier localization brought about by Coulombic scattering.^[64–67] More details and discussions can be found in the literature.^[68]

5. Applications

5.1. Self-Powered Liquid Sensors

Li et al. first proposed a microfluidic sensor by the L-TENG device,^[37] as shown in **Figure 11a**. It can be used to in situ measure the flow velocity in a microfluidic device. And it is demonstrated to serve as a self-powered chemical sensor to sense temperature, metal ion concentration, as well as the polarity parameter of the liquid online, in the micrototal analysis system, useful for controlling the results of chemical reactions. Chen et al. presented a capillary-tube L-TENG, which shows a high sensitivity to detect a 0.5 μL liquid droplet^[38] (**Figure 11b**). By the combination of the streaming potential and a graphene-based field effect transistor (FET), Newaz et al. also demonstrated a sensor, detecting the ion concentration and the velocity of the liquid flowing through the FET^[39] (**Figure 11c**). It is found that a flow rate of 70 nL min^{-1} and an ion concentration of $40 \times 10^{-9} \text{ M}$ can be detected by the sensor. Other sensing

applications in microfluids can be found in the literature.^[69,70] Since the liquid is highly mobile, Yang and co-workers report a self-powered and highly sensitive acceleration sensor based on a L-TENG composed of a liquid metal mercury droplet and nanofiber-networked film.^[40] Due to the liquid metal's high surface tension, mass density, and mobility, the sensor's output voltage and current reach up to 15.5 V and 300 nA, at an acceleration about 60 m s^{-2} , with a size of $30 \times 30 \times 6 \text{ mm}$. And it shows a linear trend as the acceleration changes, with a sensitivity of $0.26 \text{ V s}^2 \text{ m}^{-1}$ and a detection range from 0 to 60 m s^{-2} . Moreover, the sensor is mounted on an automotive engine and outputs 2.5 V as the car starts.

5.2. Wearable Power Generation

Owing to the water's deformability, the water-based nanogenerator could serve as a wearable and portable power source.^[71] **Figure 12a,b** shows two liquid-based TENGs, by using the liquid as the induction electrode. As we discussed above, the one in **Figure 12a** is flexible and maintain the output performance even under a strain as large as 300%. Yi et al. developed it as a wearable power source or a biomechanical sensor.^[43] They fabricated a bracelet-like device, worn on human's wrist, to harvest the tapping motion. The device can light up more than 80 LEDs, and charge a $1 \mu\text{F}$ capacitor as quickly as 25 V min^{-1} . Lee and co-workers fabricated a wearable L-TENG, as shown in **Figure 12b**. The textile-like device outputs a wide range from 0.5 to 2.5 Hz. After connection with a power management circuit, the device can power up a pedometer, calculator, and an electronic watch under human motions.^[44]

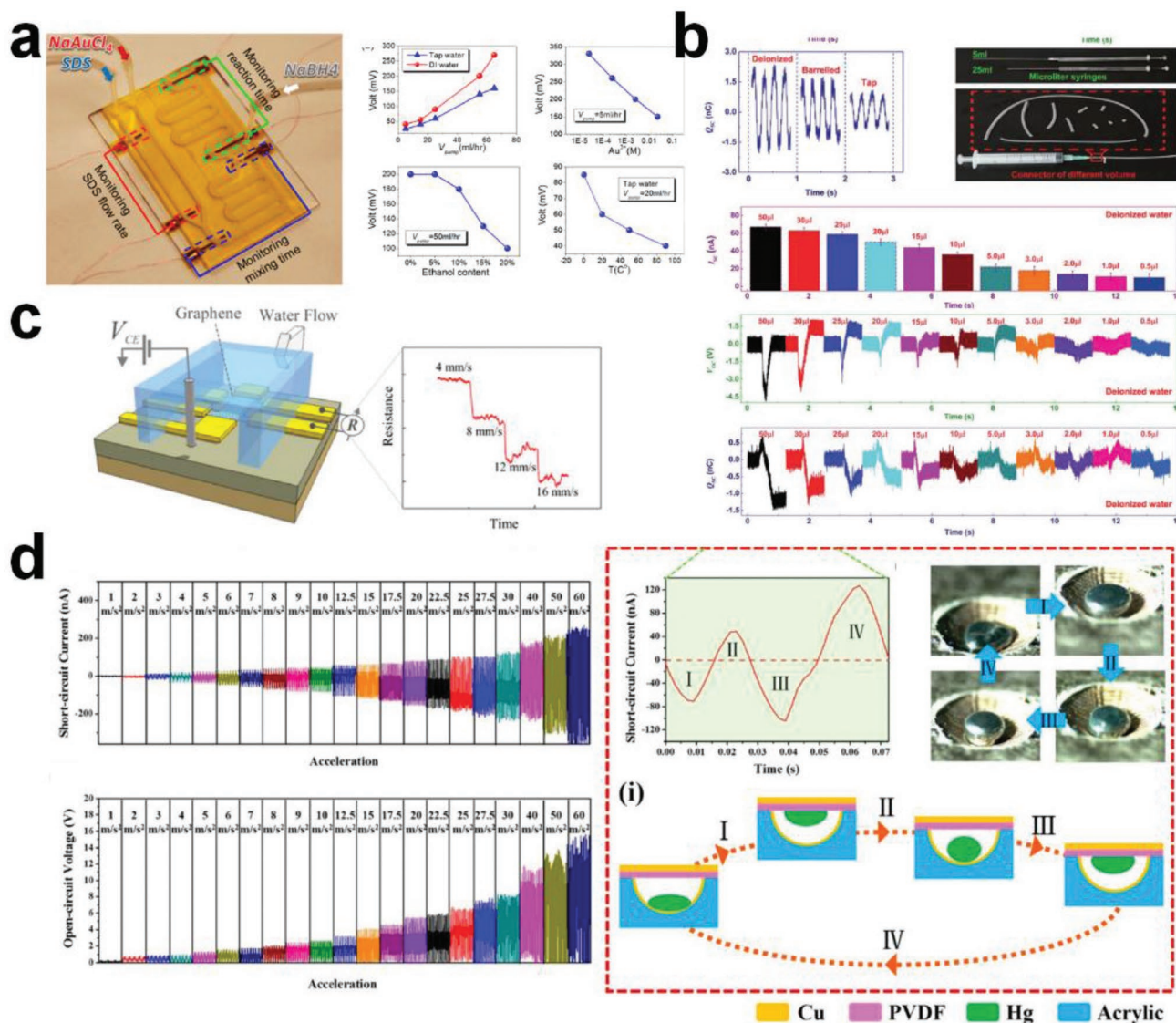


Figure 11. a,b) Self-powered microfluidic sensors. Reproduced with permission.^[37] Copyright 2015, American Chemical Society. Reproduced with permission.^[38] Copyright 2017, Wiley-VCH. c) Microfluidic sensor with the streaming current as a probe based on a graphene transistor. Reproduced with permission.^[39] Copyright 2012, American Chemical Society. d) Inertial sensor by employ a L-TENG. Reproduced with permission.^[40] Copyright 2017, American Chemical Society.

5.3. All-Weather Power Generation—Hybrid Energy Harvester

To harvest the natural water's kinetic energy, Zheng et al. proposed a hybridized cell, by integrating a solar panel with a L-TENG, which is made up of transparent materials^[46] (Figure 13a). Therefore, whether it is sunny or rainy, the cell can generate power continuously. It is found that the solar cell outputs a voltage of 0.6 V, and a current density of 350 A m^{-2} , under full Sun illumination. And the L-TENG outputs 30 V and 4.2 mA m^{-2} , under a drop dripping rate of 0.116 mL s^{-1} . To further improve the device's performance. Zheng et al. integrated a contact–separation-mode TENG inside.^[50] Then, the wind's kinetic energy is harvested (Figure 13b). It is found the output power can reach 8 mW m^{-2} at a wind speed of 2.7 m s^{-1} . Additionally, Kim's group introduced natural lotus leaf surface

to the L-TENG^[72] (Figure 13c). They employed thermal nano-imprinting with a Ni stamp, which is simple and cost-effective, to transfer the lotus leaf's superhydrophobic surface to the FEP film. This method makes the device self-cleaning and shows sustained output performance even after 1 month of exposure in the external dusty weather. Furthermore, Zhou et al. found that the water's evaporation from the carbon black sheet can generate a sustained voltage of 1 V.^[62] Therefore, we can construct an all-weather generator, no matter it is sunny, windy, rainy, or dusty.

5.4. Harvesting Water Wave Energy in Ocean—The Blue Energy

As ocean covers more than 70% of the Earth's surface, harvesting energy from the ocean is renewable and inexhaustible,

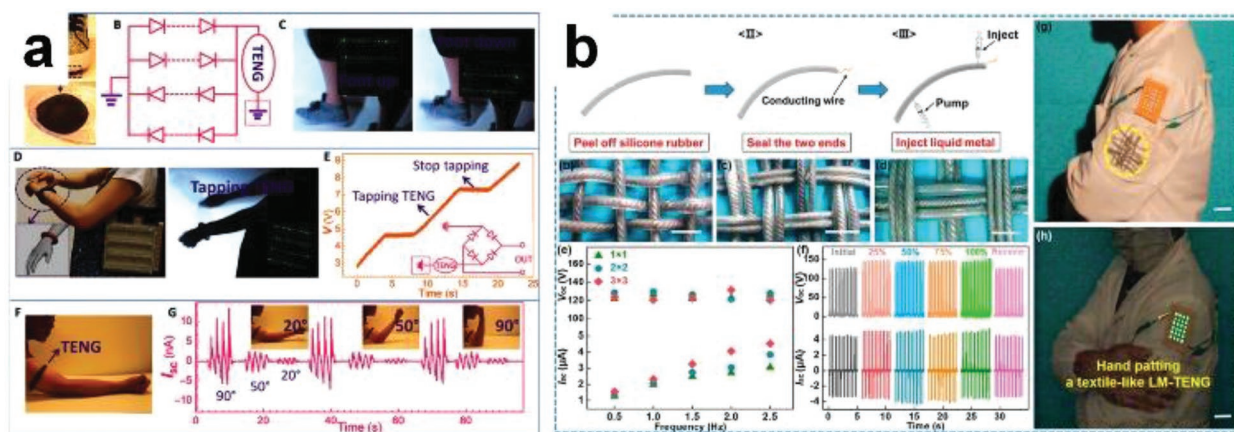


Figure 12. L-TENGs are applied as wearable power source: a) serving as a hand wrist and b) serving as a part of cloth. Reproduced under the terms and conditions of the Creative Commons Attribution-NonCommercial License.^[43] Copyright 2016, The Authors, published by AAAS. Reproduced with permission.^[44] Copyright 2018, American Chemical Society.

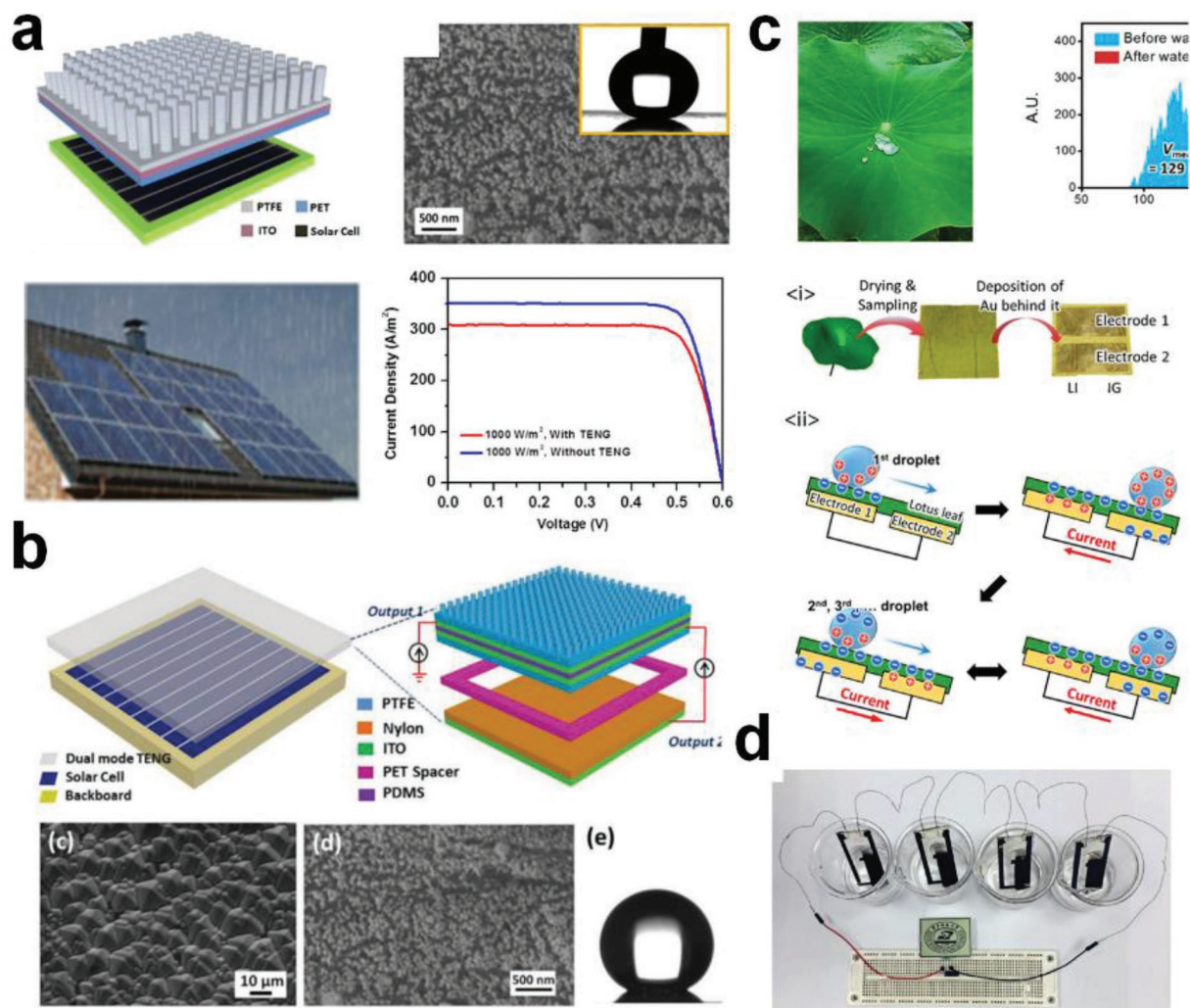


Figure 13. a) A hybrid generator for simultaneously harvesting solar energy and rain drop energy. Reproduced with permission.^[46] Copyright 2014, Elsevier. b) A hybrid generator for solar, wind and rain drop energy. Reproduced with permission.^[50] Copyright 2015, Wiley-VCH. c) A self-cleaning rain drop harvester inspired by the lotus leaf in nature. Reproduced with permission.^[72] Copyright 2017, Elsevier. d) Water-evaporation generator. Reproduced with permission.^[62] Copyright 2017, Springer Nature.

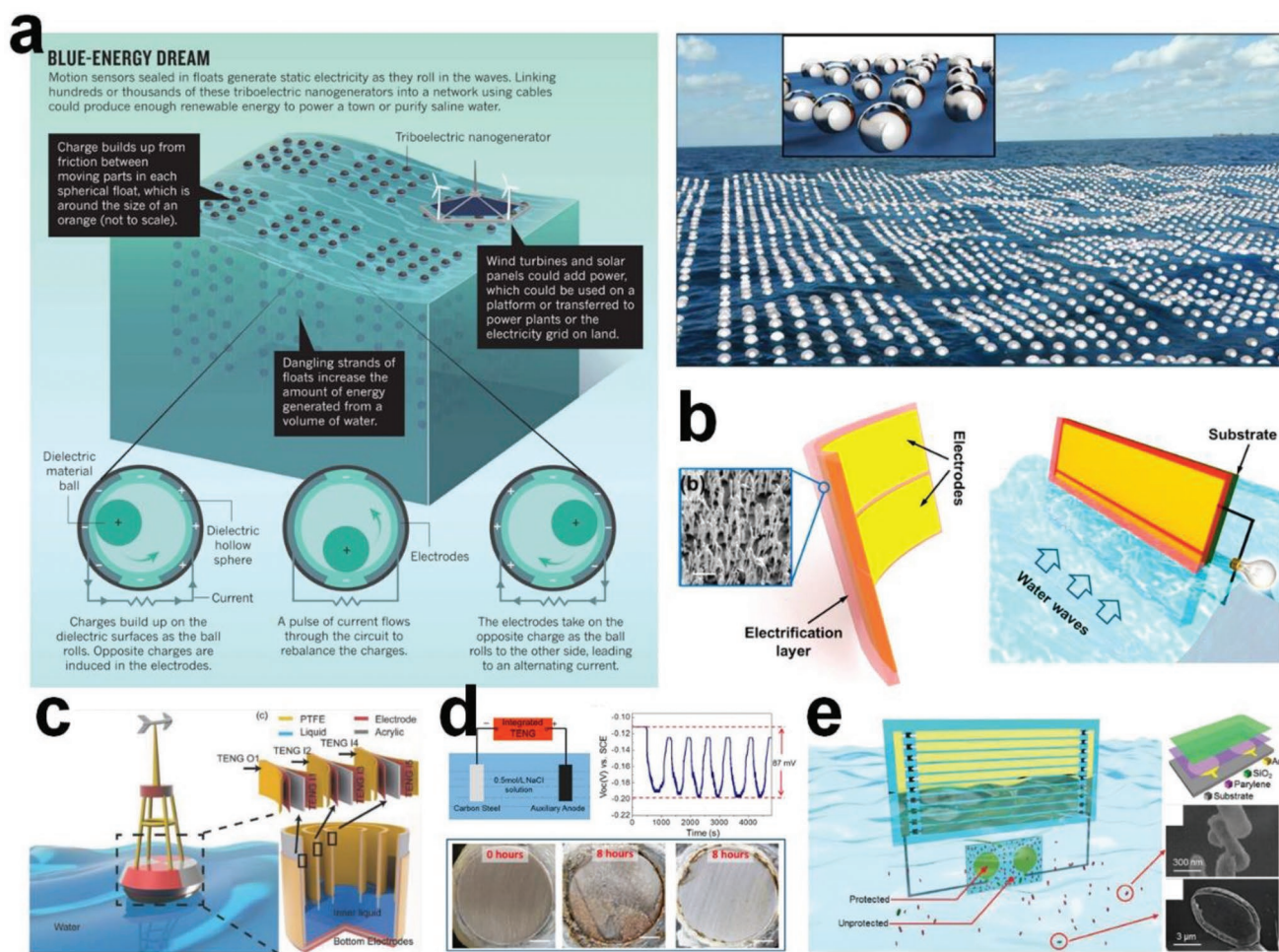


Figure 14. a) Blue energy dream using floating nets of nanogenerator. Reproduced with permission.^[51] Copyright 2017, Macmillan Publishers Limited. Reproduced with permission.^[74] Copyright 2017, Elsevier b) Nanostructured hydrophobic thin-film wave energy harvester. Reproduced with permission.^[47] Copyright 2014, American Chemical Society. c) Buoy-like TENG. Reproduced with permission.^[53] Copyright 2018, Wiley-VCH. L-TENG applied in the ocean for d) metal's cathodic protection and e) biocide-free antifouling. Reproduced with permission.^[41] Copyright 2015, American Chemical Society. Reproduced with permission.^[42] Copyright 2016, Wiley-VCH.

called as blue energy.^[51] The present commercial harvesting strategy is based on the salinity difference of the water, which is originated from the thermal energy, and locates at some estuaries.^[73] Wang et al. proposed a radically different way by using a floating networks of triboelectric nanogenerators (Figure 14a).^[51,74] It is predicted that 1000 devices spaced at 10 cm intervals in a cubic meter would power a lightbulb, and a square kilometer could generate enough electricity for a town. Besides, owing to the multiple working modes, other types of L-TENGs targeting for blue energy have been developed. Zhu et al. showed a thin film L-TENG (Figure 8b) for water wave energy harvesting.^[47] It outputs 160 V and 3 μ A. Figure 8c shows a large device, working as a buoy, with a high performance.^[53] It consists of six TENGs (one outside, five inside, as shown in Figure 8d), with a diameter around 15 cm and a height around 10 cm. All of them works in the freestanding mode. The output of a network of 18 devices are 290 μ A, 16.7 μ C, and 300 V. It is reported to power up a wireless SOS signal sending system for an ocean emergency.

Another exploiting solution for blue energy is utilizing it in situ. Zhu and co-workers demonstrated the in situ self-powered electrochemical protection system for facilities those placed in the water or the ocean.^[41,42] Figure 14e shows a corrosion protection system, based on the thin-film TENG. The electricity generated is connected to the metal that immersed in 0.5 M NaCl solution, serving as a cathodic protection strategy. It is found that the carbon steel's open-circuit potential is lowered from -111 to -198 mV. And after 4 h, the steel without protection has severe corrosion, but the one with protection shows none, proving the effectiveness of the in situ self-powered protection system. Similarly, this concept is suitable for antibiofouling, as shown in Figure 14f. It is found that, after 48 h, the unprotected surface, exposed to benthic diatom, is heavily fouled with a coverage of 79.6%, whereas this value decreases to 3.1% when the protection is applied. As the time increases to 84 h, the antiadhesion efficiency reaches to 94.6%. More discussions about the blue energy can be found in a systematical review work.^[74]

6. Summary and Perspectives

In this review, recent progresses in harvesting water energy with the advanced nanotechnology is presented. The streaming current, either in channels or on thin films, shows a good development. However, these devices are limited by the flux and the ionic concentration. The strategy to scale up the device's output with high integration still needs continuous efforts. Definitely, based on the water–solid contact electrification, the L-TENG shows probably the highest output power and wide application fields. Since the first publication on the L-TENG by Lin and Wang, researchers all over the world, including USA, China, Korea, Norway, etc., are focusing on this field. These devices are capable of serving as fluidic sensors, inertial sensors, and portable/wearable power sources. By combing with a traditional solar panel, it can realize all-weather power generation, no matter it is sunny, windy, rainy, or even dusty. Furthermore, by constructing a network of nanogenerators, such as floating ball TENGs, or underwater devices, we are promisingly to capture the blue energy, not only from the surface (wave energy), but also under the sea.

Striving toward the development of the L-TENG and its future applications, the following research aspects need to be considered and more work should be focused in order to address certain issues and constraints:

1. Developing a high charge density by water–solid contact electrification. The extended understanding of the mechanism of charge transfer between the liquid and the solid will facilitate the optimization work.
2. The gas molecule's influence on the water–solid contact electrification. In virtue of Atomic Force Microscopy and atmosphere-controllable chamber will be a promising and meaningful research direction.
3. The relationship between the water–solid contact electrification and the electric double layer need be further investigated. Since the EDL is a key component in energy storage for supercapacitors, utilizing it for energy harvesting will be very interesting.

Acknowledgements

Research was supported by the National Key R&D Project from Minister of Science and Technology (Grant No. 2016YFA0202704), National Natural Science Foundation of China (Grant Nos. 61504009, 51432005, and 5151101243), Beijing Municipal Science and Technology Commission (Grant Nos. Z171100000317001, Z171100002017017, Y3993113DF), and Youth Innovation Promotion Association, CAS.

Conflict of Interest

The authors declare no conflict of interest.

Keywords

nanogenerator, water–solid contact

Received: February 2, 2019
Revised: February 25, 2019
Published online:

- [1] H. Wendt, *Electrochemical Hydrogen Technologies-Electrochemical Production and Combustion of Hydrogen*, Elsevier, Amsterdam **1990**, p. 1.
- [2] S. U. Khan, M. Al-Shahry, W. B. Ingler, *Science* **2002**, 297, 2243.
- [3] S. Leob, R. S. Norman, *Science* **1975**, 189, 654.
- [4] Z. Lin, G. Cheng, L. Lin, S. Lee, Z. L. Wang, *Angew. Chem., Int. Ed.* **2013**, 52, 12545.
- [5] F. R. Fan, Z. Q. Tian, Z. L. Wang, *Nano Energy* **2012**, 1, 328.
- [6] S. Wang, L. Lin, Z. L. Wang, *Nano Lett.* **2012**, 12, 6339.
- [7] S. Wang, L. Lin, Z. L. Wang, *Nano Energy* **2015**, 11, 436.
- [8] Z. L. Wang, J. Song, *Science* **2006**, 312, 242.
- [9] Z. L. Wang, *Mater. Today* **2017**, 20.
- [10] Z. L. Wang, *ACS Nano* **2013**, 7, 9533.
- [11] W. Tang, B. Meng, H. X. Zhang, *Nano Energy* **2013**, 2, 1164.
- [12] K. Lee, M. Gupta, S. Kim, *Nano Energy* **2015**, 14, 139.
- [13] L. Lin, S. Wang, Y. Xie, Q. Jing, S. Niu, Y. Hu, Z. L. Wang, *Nano Lett.* **2013**, 13, 2916.
- [14] G. Yao, L. Kang, J. Li, Y. Long, H. Wei, C. A. Ferreira, J. J. Jeffery, Y. Lin, W. Cai, X. Wang, *Nat. Commun.* **2018**, 9, 5349.
- [15] R. Hinchet, S. Kim, *ACS Nano* **2015**, 9, 7742.
- [16] Z. L. Wang, J. Chen, L. Lin, *Energy Environ. Sci.* **2015**, 8, 2250.
- [17] S. Kim, M. K. Gupta, K. Y. Lee, A. Sohn, T. Y. Kim, K.-S. Shin, D. Kim, S. K. Kim, K. H. Lee, H.-J. Shin, D.-W. Kim, S.-W. Kim, *Adv. Mater.* **2014**, 26, 3918.
- [18] C. K. Jeong, K. M. Baek, S. Niu, T. W. Nam, Y. H. Hur, D. Y. Park, G. T. Hwang, M. Byun, Z. L. Wang, Y. S. Jung, K. J. Lee, *Nano Lett.* **2014**, 14, 7031.
- [19] S. Park, H. Kim, M. Vosgueritchian, S. Cheon, H. Kim, J. H. Koo, T. R. Kim, S. Lee, G. Schwartz, H. Chang, Z. Bao, *Adv. Mater.* **2014**, 26, 7324.
- [20] J. Xiong, P. Cui, X. Chen, J. Wang, K. Parida, M. F. Lin, P. S. Lee, *Nat. Commun.* **2018**, 9, 4280.
- [21] B. Meng, W. Tang, X. Zhang, M. Han, W. Liu, H. Zhang, *Nano Energy* **2013**, 2, 1101.
- [22] Y. Lee, S. H. Cha, Y. Kim, D. Choi, J. Y. Sun, *Nat. Commun.* **2018**, 9, 1804.
- [23] M. Li, A. L. Porter, Z. L. Wang, *Nano Energy* **2017**, 34, 93.
- [24] Y. Zi, S. Niu, J. Wang, Z. Wen, W. Tang, Z. L. Wang, *Nat. Commun.* **2015**, 6, 8376.
- [25] Y. Long, Y. Yu, X. Yin, J. Li, C. Carlos, X. Du, Y. Jiang, X. D. Wang, *Nano Energy* **2018**, 57, 558.
- [26] W. Li, D. Torres, R. Díaz, Z. Wang, C. Wu, C. Wang, Z. L. Wang, N. Sepúlveda, *Nat. Commun.* **2017**, 8, 15310.
- [27] K. Y. Lee, J. Chun, J. Lee, K. N. Kim, N. Kang, J. Kim, M. H. Kim, K. Shin, M. K. Gupta, J. M. Baik, S. Kim, *Adv. Mater.* **2014**, 26, 5037.
- [28] J. Chun, B. Uk Ye, J. W. Lee, D. Choi, C. Y. Kang, S. W. Kim, Z. L. Wang, J. M. Baik, *Nat. Commun.* **2016**, 7, 12985.
- [29] G. Quincke, *Ann. Phys. Chem.* **1859**, 183, 1.
- [30] A. E. Cohen, *Science* **2003**, 300, 1235.
- [31] F. H. J. van der Heyden, D. Stein, C. Dekker, *Phys. Rev. Lett.* **2005**, 95, 116104.
- [32] R. Zhang, S. Wang, M. Yeh, C. Pan, L. Lin, R. Yu, Y. Zhang, L. Zheng, Z. Jiao, Z. L. Wang, *Adv. Mater.* **2015**, 27, 6482.
- [33] R. Liu, C. Liu, S. Fan, *ACS Appl. Mater. Interfaces* **2018**, 10, 35273.
- [34] J. Yin, Z. Zhang, X. Li, J. Yu, J. Zhou, Y. Chen, W. Guo, *Nat. Commun.* **2014**, 5, 3582.
- [35] S. Yang, Y. Su, Y. Xu, Q. Wu, Y. Zhang, M. B. Raschke, M. Ren, Y. Chen, J. Wang, W. Guo, Y. Shen, C. Tian, *J. Am. Chem. Soc.* **2018**, 140, 13746.
- [36] J. Yin, X. Li, J. Yu, Z. Zhang, J. Zhou, W. Guo, *Nat. Nanotechnol.* **2014**, 9, 378.
- [37] X. Li, M. H. Yeh, Z. H. Lin, H. Guo, P. K. Yang, J. Wang, S. Wang, R. Yu, T. Zhang, Z. L. Wang, *ACS Nano* **2015**, 9, 11056.
- [38] B. D. Chen, W. Tang, C. He, T. Jiang, L. Xu, L. P. Zhu, G. Q. Gu, J. Chen, J. J. Shao, J. Luo, Z. L. Wang, *Adv. Mater. Tech.* **2017**, 3, 1700229.

- [39] A. K. M. Newaz, D. A. Markov, D. Prasai, K. I. Bolotin, *Nano Lett.* **2012**, *12*, 2931.
- [40] B. Zhang, L. Zhang, W. Deng, L. Jin, F. Chun, H. Pan, B. Gu, H. Zhang, Z. Lv, W. Yang, Z. L. Wang, *ACS Nano* **2017**, *11*, 7440.
- [41] X. J. Zhao, G. Zhu, Y. J. Fan, H. Y. Li, Z. L. Wang, *ACS Nano* **2015**, *9*, 7671.
- [42] X. J. Zhao, J. J. Tian, S. Y. Kuang, H. Ouyang, L. Yan, Z. L. Wang, Z. Li, G. Zhu, *Adv. Mater. Interfaces* **2016**, *3*, 1600187.
- [43] F. Yi, X. Wang, S. Niu, S. Li, Y. Yin, K. Dai, G. Zhang, L. Lin, Z. Wen, H. Guo, J. Wang, M. H. Yeh, Y. Zi, Q. Liao, Z. You, Y. Zhang, Z. L. Wang, *Sci. Adv.* **2016**, *2*, e1501624.
- [44] Y. Yang, N. Sun, Z. Wen, P. Cheng, H. Zheng, H. Shao, Y. Xia, C. Chen, H. Lan, X. Xie, C. Zhou, J. Zhong, X. Sun, S. T. Lee, *ACS Nano* **2018**, *12*, 2027.
- [45] Z. H. Lin, G. Cheng, S. Lee, K. C. Pradel, Z. L. Wang, *Adv. Mater.* **2014**, *26*, 4690.
- [46] L. Zheng, Z. H. Lin, G. Cheng, W. Wu, X. Wen, S. Lee, Z. L. Wang, *Nano Energy* **2014**, *9*, 291.
- [47] G. Zhu, Y. Su, P. Bai, J. Chen, Z. L. Wang, *ACS Nano* **2014**, *8*, 6031.
- [48] X. Zhao, S. Y. Kuang, Z. L. Wang, G. Zhu, *ACS Nano* **2018**, *12*, 4280.
- [49] Y. Xi, J. Wang, Y. Zi, X. Li, C. Han, X. Cao, C. Hu, Z. L. Wang, *Nano Energy* **2017**, *38*, 101.
- [50] L. Zheng, G. Cheng, J. Chen, L. Lin, J. Wang, Y. Liu, H. Li, Z. L. Wang, *Adv. Energy Mater.* **2015**, *5*, 1501152.
- [51] Z. L. Wang, *Nature* **2017**, *542*, 159.
- [52] C. Wu, A. C. Wang, W. Ding, H. Guo, Z. L. Wang, *Adv. Energy Mater.* **2018**, 1802906.
- [53] X. Li, J. Tao, X. Wang, J. Zhu, C. F. Pan, Z. L. Wang, *Adv. Energy Mater.* **2018**, *8*, 1800705.
- [54] W. Tang, T. Jiang, F. R. Fan, A. F. Yu, C. Zhang, X. Cao, Z. L. Wang, *Adv. Funct. Mater.* **2015**, *25*, 3718.
- [55] J. Chen, W. Tang, C. Lu, L. Xu, Z. Yang, B. Chen, Z. L. Wang, *Appl. Phys. Lett.* **2017**, *110*, 201603.
- [56] B. Ravelo, F. Duval, S. Kane, B. Nsom, *J. Electrostat.* **2011**, *69*, 473.
- [57] T. Takahashi, *Rev. Geophys.* **1973**, *11*, 903.
- [58] S. K. Banerji, S. R. Lele, *Nature* **1932**, *13*, 2226.
- [59] J. Chen, H. Guo, J. Zheng, Y. Huang, G. Liu, C. G. Hu, Z. L. Wang, *ACS Nano* **2016**, *10*, 8104.
- [60] W. Olthuis, B. Schippers, J. Eijkel, A. Berg, *Sens. Actuators, B* **2005**, *111–112*, 385.
- [61] E. Donath, A. Voigt, *J. Colloid Interface Sci.* **1986**, *109*, 122.
- [62] G. Xue, Y. Xu, T. Ding, J. Li, J. Yin, W. Fei, Y. Cao, J. Yu, L. Yuan, L. Gong, J. Chen, S. Deng, J. Zhou, W. Guo, *Nat. Nanotechnol.* **2017**, *12*, 317.
- [63] L. E. Helseth, *Nano Energy* **2018**, *50*, 266.
- [64] P. Král, M. Shapiro, *Phys. Rev. Lett.* **2001**, *86*, 131.
- [65] S. Ghosh, A. K. Sood, N. Kumar, *Science* **2003**, *299*, 1042.
- [66] B. N. J. Persson, U. Tartaglino, E. Tosatti, H. Ueba, *Phys. Rev. B* **2004**, *69*, 235410.
- [67] H. Helmholtz, *Ann. Phys. Chem.* **1879**, *243*, 337.
- [68] A. T. Liu, G. Zhang, A. L. Cottrill, Y. Kunai, A. Kaplan, P. Liu, V. B. Koman, M. S. Strano, *Adv. Energy Mater.* **2018**, *8*, 1802212.
- [69] X. Zhang, Y. Zheng, D. Wang, F. Zhou, *Nano Energy* **2017**, *40*, 95.
- [70] W. Kim, D. Choi, J.-Y. Kwon, D. Choi, *J. Mater. Chem. A* **2018**, *6*, 14069.
- [71] F. R. Fan, W. Tang, Z. L. Wang, *Adv. Mater.* **2016**, *28*, 4283.
- [72] D. Choi, D. W. Kim, D. Yoo, K. J. Cha, M. La, D. S. Kim, *Nano Energy* **2017**, *36*, 250.
- [73] Z. Jia, B. Wang, S. Song, Y. Fan, *Renewable Sustainable Energy Rev.* **2014**, *31*, 91.
- [74] Z. L. Wang, T. Jiang, L. Xu, *Nano Energy* **2017**, *39*, 9.